

Letters

Block-by-Block Growth of Single-Crystalline Si/SiGe Superlattice Nanowires

Yiying Wu, Rong Fan, and Peidong Yang*

*Department of Chemistry, University of California, Materials Science Division, Lawrence Berkeley National Laboratory, Berkeley, California 94720**Received December 3, 2001; Revised Manuscript Received December 23, 2001*

ABSTRACT

Heterojunction and superlattice formation is essential for many potential applications of semiconductor nanowires in nanoscale optoelectronics. We have developed a hybrid pulsed laser ablation/chemical vapor deposition (PLA-CVD) process for the synthesis of semiconductor nanowires with longitudinal ordered heterostructures. The laser ablation process generates a programmable pulsed vapor source, which enables the nanowire growth in a block-by-block fashion with a well-defined compositional profile along the wire axis. Single-crystalline nanowires with longitudinal Si/SiGe superlattice structure have been successfully synthesized. This unique class of heterostructured one-dimensional nanostructures holds great potential in applications such as light emitting devices and thermoelectrics.

The success of semiconductor integrated circuits has been largely hinged upon the capability of heterostructure formation through carefully controlled doping and interfacing. In fact, the 2-dimensional (2D) semiconductor interface is ubiquitous in optoelectronic devices such as light emitting diode, laser diodes, quantum cascade lasers, and transistors. Heterostructure formation in 1-dimensional (1D) nanostructures (nanowires) is equally important for their potential applications as efficient light emitting sources and better thermoelectrics.^{1–9} While there are a number of well-developed techniques (e.g., molecular beam epitaxy) for the fabrication of thin film heterostructures and superlattices, a general synthetic scheme for heterojunction and superlattice formation in 1D nanostructures with well-defined coherent interfaces is currently still lacking. Previous studies on

semiconductor nanowires or nanotubes have invariably dealt with homogeneous systems with a few exceptions of heterostructure formation including heterojunctions between carbon nanotubes and silicon/carbide nanowires,^{10,11} and p–n junction on individual carbon nanotubes¹² or GaAs/Ga_{1–x}In_xAs nanowires.^{13,14} Recently, a sequential electrochemical method was reported to synthesize metal bar-coded micro-rods.^{9,15} This method, however, yields polycrystalline products with less than ideal interfaces. Here, we report a hybrid pulsed laser ablation/chemical vapor deposition (PLA-CVD) process for the synthesis of semiconductor nanowires with periodic longitudinal heterostructures. Single-crystalline nanowires with Si/SiGe superlattice structure are obtained and thoroughly characterized using electron microscopy.

Figure 1a shows our nanowire growth apparatus. A (111) Si wafer coated with a thin layer of Au was put inside a

* Corresponding author. Email: p_yang@uclink.berkeley.edu

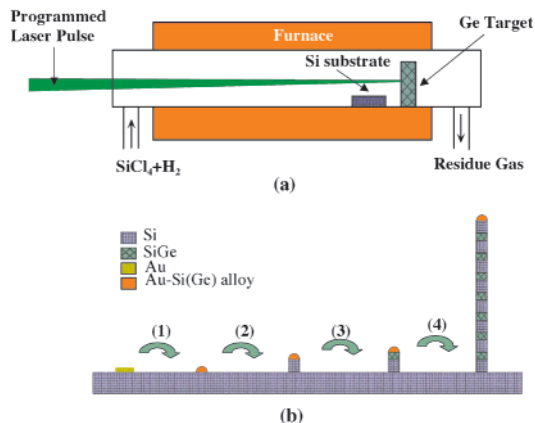


Figure 1. Schematic illustration of the experimental setup (a) and vapor–liquid–solid sequential nanowire growth mechanism (b). Figure (b) shows different stages of the block-by-block nanowire growth process: (1) alloying process between Au thin film and Si species in substrate/vapor; (2) growth of pure Si block when the laser is off, only Si species deposit into the alloy droplet; (3) growth of SiGe alloy block when the laser is on, both Si and Ge species deposit into the liquid droplet; (4) growth of Si/SiGe superlattice structure by turning on and off the laser beam periodically. During the experiment, the flow rate of H_2 is 100 sccm, the ratio of $SiCl_4$ and H_2 is 0.02 and the system pressure is at one atmosphere. The laser beam is focused on the target with an energy density of $10 J/cm^2$ per pulse.

quartz furnace tube as substrate. A gas mixture of H_2 and $SiCl_4$ was continuously introduced into the reaction tube. Nanowire growth is based on the well-known vapor–liquid–solid (VLS) mechanism (Figure 1b) with Au as solvent at high temperature.^{16–19} This process starts with the dissolution of gaseous reactants in nanosized liquid droplets of the metal solvent, followed by nucleation and growth of single

crystalline wires (Figure 1b). The concept of heterostructured nanowires requires accurate compositional profile and interface control at the nanometer or even atomic level while maintaining a highly crystalline and coherent interface along the wire axis. Based on our fundamental mechanistic understanding of VLS nanowire growth,¹⁸ this level of control is made possible here through successive feed-in of different vapor sources. To synthesize Si/SiGe superlattice nanowires, Ge vapor was generated in pulsed form through the pulsed ablation of a pure Ge target with a frequency-doubled Nd:YAG laser (wavelength 532 nm, 6 Hz, power density $10 J/cm^2$ per pulse). The reaction temperature typically ranged from $850\text{ }^\circ\text{C}$ to $950\text{ }^\circ\text{C}$. At this temperature, a Au thin film forms a liquid alloy with Si and spontaneously breaks up into nanometer sized droplets (Figure 1b (1)). Si species continuously deposit into Au–Si alloy droplets where the Si nanowire growth is initiated upon supersaturation (Figure 1b (2)). During this growth process, if the laser is turned on, Ge vapor will be generated and both Ge and Si species will be deposited into the alloy droplets. The SiGe alloy then precipitates from the solid/liquid interface (Figure 1b (3)). By periodically turning the laser on and off (this sequence can be readily programmed), Si/SiGe superlattice is formed on every individual nanowire (Figure 1b (4)) in a block-by-block fashion. The entire growth process resembles the living polymerization synthesis of block copolymer.

Figure 2a shows a scanning electron microscopy (SEM) image of the synthesized nanowire array. For this sample, the Au film thickness on Si (111) substrate was 20 nm. During the growth process, the laser was periodically turned on for 5 s and off for 25 s, and the cycle was repeated for 15 min. As previously shown, Si nanowires grow preferably along the [111] direction,¹⁹ which results in the oriented

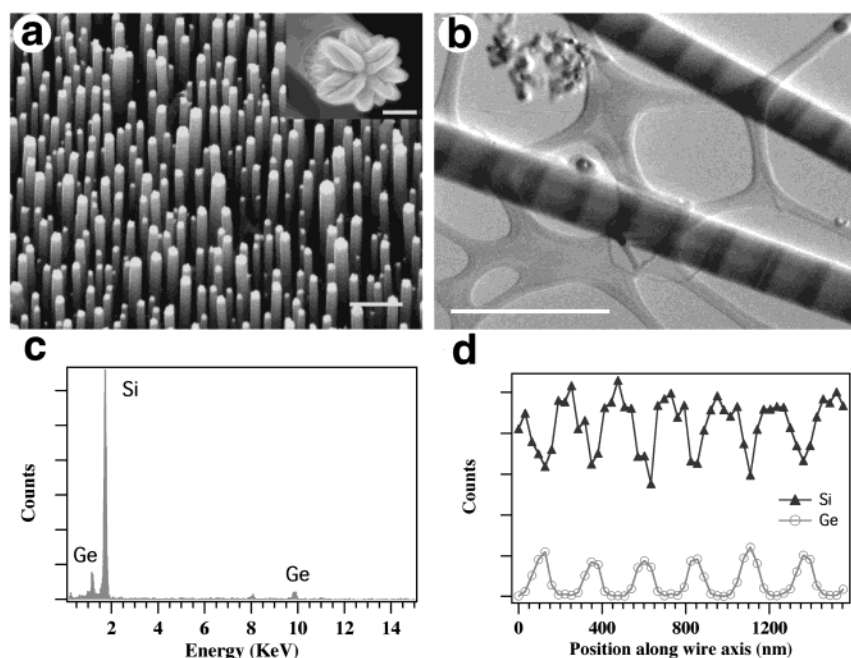


Figure 2. (a) SEM image of the heterostructured nanowire array on Si (111) substrate. The scale bar is $1\text{ }\mu\text{m}$. The inset shows the tip of one nanowire. The scale bar is 100 nm. (b) STEM image of two nanowires in bright field mode. The scale bar is 500 nm. (c) EDS spectrum of the Ge rich region on Si/SiGe superlattice nanowires. (d) Line profile of EDS signal from Si and Ge components along the nanowire growth axis. The experiments were carried out on a Philip CM200 TEM operated at 200 keV.

epitaxial nanowire array growth on the Si (111) substrate. The alloy droplet solidifies and appears as a bright spot on the tip of every nanowire. The inset of Figure 2a shows a close view of the tip with a flower-like shape, which is formed during the solidification of the liquid alloy droplet. The diameters of these nanowires range from 50 to 300 nm. Figure 2b shows a scanning transmission electron microscopy (STEM) image of two nanowires in bright-field mode. Along the wire axes, dark stripes appear periodically, which originate from the periodic deposition of the SiGe alloy and Si segments. The electron scattering cross section of the Ge atom is larger than that of Si. Consequently, the SiGe alloy block appears darker than the pure Si block. The chemical composition of the darker area is examined using energy-dispersive X-ray spectroscopy (EDS) (Figure 2c), which shows a strong Si peak and apparent Ge doping (~12 wt % Ge). The periodic modulation of Ge doping is further confirmed by scanning a focused electron beam along the nanowire growth axis and tracking the change of X-ray signal from Si and Ge atoms in the wires (Figure 2d). Both Si and Ge X-ray signals show periodic modulation, and their intensities are anticorrelated: wherever the X-ray signal from Ge shows a maximum, the signal from Si shows a minimum, which confirms the formation of Si/SiGe superlattice along the wire axis. We note that the abruptness of the Si/SiGe interface in these nanowires is not ideal at this stage. It is believed that this could be improved by incorporating more precise and faster vapor dosing/switching schemes such as molecular beam processes.

It must be emphasized that the elastic boundary conditions of VLS nanowire heteroepitaxial growth offer the possibility to create dislocation-free interfaces in the superlattice nanowires that are not stable in the conventional 2D configuration achieved by epitaxial film growth on planar substrates. Although coherent heteroepitaxial films can be grown well beyond the equilibrium critical thickness, the films are metastable to relaxation by dislocation mechanisms. The VLS nanowire morphology provides an opportunity to markedly extend both the equilibrium and kinetic critical thicknesses, or equivalently, the lattice misfit that can be accommodated at a given thickness, due to the change in boundary conditions. The highly crystalline nature of our superlattice nanowires is characterized by selected area electron diffraction (SAED) and high-resolution transmission electron microscopy (HRTEM). Figure 3 inset shows an SAED pattern, recorded perpendicular to a nanowire long axis. The pattern can be indexed as the diffraction along the [110] zone axis of crystalline Si and suggests the nanowire growth does occur along [111] direction. This is further confirmed in the HRTEM image (Figure 3), which clearly shows the (111) atomic planes (separation 0.314 nm) perpendicular to the nanowire axis. While the interface contrast can be readily seen in the STEM images (Figure 2a), we were not able to resolve the interface in HRTEM mode due to low doping percentage in SiGe blocks. These HRTEM images, however, clearly demonstrate the high crystallinity of the Si/SiGe superlattice nanowires. Extensive HRTEM imaging indicates that the monocrystallinity of the Si/SiGe superlattice nano-

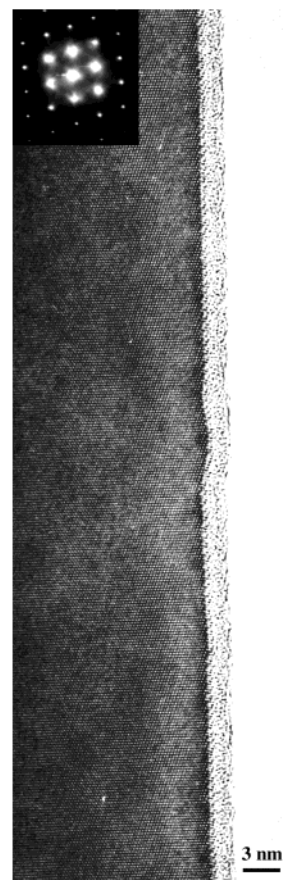


Figure 3. HRTEM image of a Si/SiGe superlattice nanowire. The inset shows a selected-area-electron-diffraction (SAED) pattern. The data were collected on an atomic resolution microscope (ARM) operated at 800 keV.

wire is maintained along the entire wire length with few linear or planar defects.

Taken together, the structural and chemical composition data show that the nanowires prepared by our PLA-CVD method are highly crystalline with Si/SiGe superlattice structure along the nanowire axis. The diameters of the nanowires, the concentration of Ge and the period of chemical modulation can be readily controlled by adjusting the reaction conditions. The nanowire diameter is influenced by the thickness of the Au layer on the substrate. With 20 nm thick Au thin films, the average diameter of nanowires is around 100 nm. If the thickness of Au is reduced to 1 nm, the average diameter can be reduced to 20 nm. The diameter is also affected by the reaction temperature. Lower temperature results in thinner nanowires. The concentration of Ge in the superlattice is controlled by the ratio of Ge atoms and Si atoms deposited into the alloy droplets. Increasing the laser intensity or decreasing the flow rate of SiCl₄ can increase the concentration of Ge. In addition, the superlattice period (L) is the product of growth rate (V) and laser on-and-off period (T): $L = V \times T$. Therefore, by reducing the growth rate or the laser on-and-off period, we are able to reduce the superlattice period. Similarly, the ratio of different compositional blocks can be readily adjusted by varying the laser on/off ratio.

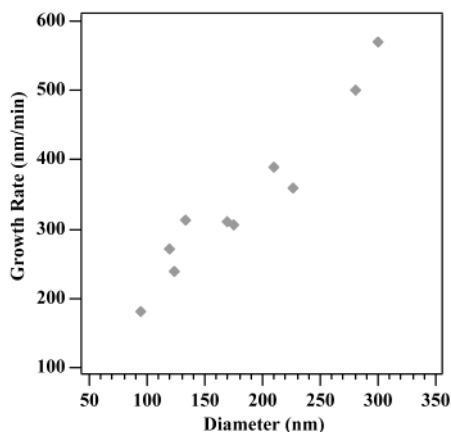


Figure 4. Correlation between the nanowire growth rate and diameter observed in one set of our experiment. During the experiment, the flow rate of H_2 is 100 sccm, the ratio of $SiCl_4$ and H_2 is 0.02, and the system pressure is at one atmosphere. The laser beam is focused on the target with an energy density of $10 J/cm^2$ per pulse. During the growth process, the laser was periodically turned on for 5 s and off for 25 s, and the cycle was repeated for 15 min.

Importantly, by putting these “labels” along the wire growth axis, the PLA-CVD process provides a quantitative way to measure the growth rate of nanowires ($V = L/T$) and its correlation with growth supersaturation. While the laser on-and-off period T is preset, knowing the superlattice period L means the growth rate V can be accurately calculated. It is found that the growth rate is diameter-dependent under the same reaction conditions. The smaller the nanowire diameter, the slower is the growth rate (Figure 4). The trend can be qualitatively explained by the Gibbs–Thomson effect, i.e., increasing Si vapor pressure and thereby decreasing supersaturation as the nanowire diameter becomes smaller. The decrease of supersaturation as a function of nanowire diameter (d) is given as

$$\frac{\Delta\mu}{kT} = \frac{\Delta\mu_0}{kT} - \frac{4\Omega\alpha_{vs}}{kT} \frac{1}{d}$$

where $\Delta\mu$ is the effective difference between the chemical potentials of Si in the nutrient (vapor or liquid) phase and in the nanowire, $\Delta\mu_0$ is the same difference at a plane interface, α_{vs} is the specific free energy of the nanowire surface and Ω is the atomic volume of Si. The dependence of the crystal growth rate V on the supersaturation is generally nonlinear and in many cases is of n th power

$$V = b \left(\frac{\Delta\mu}{kT} \right)^n$$

where b is a coefficient independent of the supersaturation. This naturally leads to a linear dependence between $V^{1/n}$ and $1/d$ as in

$$\sqrt[n]{V} = \frac{\Delta\mu_0}{kT} \sqrt[n]{b} - \frac{4\Omega\alpha_{vs}}{kT} \sqrt[n]{b} \frac{1}{d}$$

Our Si/SiGe nanowire growth data can be readily fitted with

$n = 2$. This observation agrees well with the classical CVD crystal growth studies on micrometer-sized Si whiskers by Givargizov.^{16–19}

The hybrid PLA-CVD method used in our experiment can be used to prepare various other heterostructures on individual nanowires in a “custom-made” fashion since part of the vapor source supplies (laser ablation) can be programmed. It will enable the creation of various functional devices (e.g., p–n junction, coupled quantum dot structure, and heterostructured bipolar transistor) on single nanowires. These nanowires could be used as important building blocks for constructing nanoscale electronic circuits and light emitting devices. As an example, superlattice nanowires with reduced phonon transport and high electron mobility are believed to be better thermoelectrics.^{20–22}

Acknowledgment. Dedicated to Professor Galen D. Stucky on the occasion of his 65th birthday. This work was supported by the Camille and Henry Dreyfus Foundation, 3M Corporation, a Career Award from the National Science Foundation, and University of California, Berkeley. P.Y. is an Alfred P. Sloan Research Fellow. Work at the Lawrence Berkeley National Laboratory was supported by the Office of Science, Basic Energy Sciences, Division of Materials Science of the U.S. Department of Energy. The authors thank C. Nelson, D. Ah Tye, and C. Song for the help in SEM and TEM experiments. We thank the National Center of Electron Microscopy for the use of their facilities.

References

- (1) Hu, J.; Odom, T. W.; Lieber, C. M. *Acc. Chem. Res.* **1999**, *32*, 435.
- (2) Wang, E. W.; Sheehan, P. E.; Lieber, C. M. *Science* **1997**, *277*, 1971.
- (3) Canham, L. T. *Appl. Phys. Lett.* **1990**, *57*, 1046.
- (4) Holmes, J. D.; Johnston, K. P.; Doty, R. C.; Korgel, B. A. *Science* **2000**, *287*, 1471.
- (5) Hicks, L. D.; Dresselhaus, M. S. *Phys. Rev.* **1993**, *B47(24)*, 16631.
- (6) Cui, Y.; Lieber, C. M. *Science* **2001**, *291*, 851.
- (7) Huang, M.; Mao, S.; Feick, H.; Yan, H.; Wu, Y.; Kind, H.; Weber, E.; Russo, R.; Yang, P. *Science* **2001**, *292*, 1897.
- (8) Favier, F.; Walter, E. C.; Zach, M. P.; Benter, T.; Penner, R. M. *Science* **2001**, *293*, 2227.
- (9) Kovtyukhova, N. I.; Martin, B. R.; Mbindyo, J. K. N.; Smith, P. A.; Razavi, B.; Mayer, T. S.; Mallouk, T. E. *J. Phys. Chem. B* **2001**, *105*, 8762.
- (10) Hu, J.; Ouyang, M.; Yang, P.; Lieber, C. M. *Nature* **1999**, *399*, 48.
- (11) Zhang, Y.; Ichihashi, T.; Landree, E.; Nihey, F.; Iijima, S. *Science* **1999**, *285*, 1719.
- (12) Zhou, C.; Kong, J.; Yenilmez, E.; Dai, H. *Science* **2000**, *290*, 1552.
- (13) Haraguchi, K.; Katsuyama, T.; Hiruma, K. *J. Appl. Phys.* **1994**, *75*, 4220.
- (14) Markowitz, P. D.; Zach, M. P.; Gibbons, P. C.; Penner, R. M.; Buhro, W. E. *J. Am. Chem. Soc.* **2001**, *123*, 4502.
- (15) Nicewarner-Pena, S.; Freeman, R. G.; Reiss, B. D.; He, L.; Pena, D. J.; Walton, I. D.; Cromer, R.; Keating, C. D.; Natan, M. J. *Science* **2001**, *294*, 137.
- (16) Wagner, R. S.; Ellis, W. C. *Appl. Phys. Lett.* **1964**, *4*, 89.
- (17) Wagner, R. S. In *Whisker Technology*; Levitt, A. P., Ed.; Wiley: New York, 1970; p 47.
- (18) Wu, Y.; Yang, P. *J. Am. Chem. Soc.* **2001**, *123*, 3165.
- (19) Givargizov, E. I. *J. Cryst. Growth* **1975**, *31*, 20.
- (20) Koga, T.; Sun, X.; Cronin, S. B.; Dresselhaus, M. S. *Appl. Phys. Lett.* **1999**, *75*, 2438.
- (21) Koga, T.; Cronin, S. B.; Dresselhaus, M. S.; Liu, J. L.; Wang, K. L. *Appl. Phys. Lett.* **2000**, *77*, 1490.
- (22) Venkatasubramanian, R.; Siivola, E.; Colpitts, T.; O’Quinn, B. *Nature* **2001**, *413*, 597.

NL0156888